

# Some Factors Influencing Exfoliation and Physical Property Enhancement in Nanoclay Epoxy Resins Based on Diglycidyl Ethers of Bisphenol A and F

S. Ingram, I. Rhoney, J. J. Liggat, N. E. Hudson, R. A. Pethrick

Department of Pure and Applied Chemistry, University of Strathclyde, Glasgow G1 1XL, United Kingdom

Received 8 June 2006; accepted 31 August 2006

DOI 10.1002/app.25474

Published online 11 June 2007 in Wiley InterScience (www.interscience.wiley.com).

**ABSTRACT:** An investigation of the factors influencing the degree of exfoliation of an organically modified clay in a series of epoxy resins is reported. The use of sonication, choice of curing agent, effect of the moisture content of the clay, and the cure temperature were examined. The dispersion was characterized using a combination of rheological measurements, X-ray diffraction, and dynamic mechanical thermal analysis. Rheological analysis of the clay dispersion in the epoxy monomer indicated that at high clay loads Herschel–Bulkley type behavior is followed. Higher

cure temperatures and higher levels of clay moisture were found to influence the extent of exfoliation. Improvements in physical properties were observed through the addition of nanocomposites. The DGEBA/DDM and DEGEBA/DDS exhibited 2 and 4°C increase, respectively, in  $T_g$  per wt % of added clay. DGEBF showed virtually no enhancement. © 2007 Wiley Periodicals, Inc. *J Appl Polym Sci* 106: 5–19, 2007

**Key words:** epoxy; nanocomposites; montmorillonite clay

## INTRODUCTION

The incorporation of silicate platelets into polymers to produce nanocomposites has attracted considerable interest in the last few years.<sup>1,2</sup> Conventional fillers have been used for many years to reduce costs and/or enhance physical properties of polymers.<sup>3,4</sup> The principle distinction between the silicate platelets and conventional fillers lies in the length scales and aspect ratios of the former relative to the latter. Layered silicate clays offer the possibility of creating a three-dimensional structure that can inhibit small molecule permeability within the matrix. Such inorganic materials are available where one of the dimensions of the particle lies in the nanometre length scale. However, organically modified smectite clays (e.g., montmorillonite and related layered silicates) are frequently the materials of choice because of the ease of dispersion of the individual exfoliated platelets in the polymer material.<sup>1,2</sup> A wide range of polymer-based nanocomposites has been reported recently and include polysiloxanes, polyurethanes, acrylic, polyamides, phenolic, and epoxy resins in addition to various thermoplastics.<sup>5–13</sup> The first studies of nanoclay composites were reported for nylon<sup>14</sup> where significant improvements

in flame retardancy, water uptake, and mechanical strength were achieved.

Clay has been added to polymers for many years, but the breakthrough in terms of physical property enhancement came with the achievement of intercalated and exfoliated states for the platelets within the matrix. In many systems, conventional clay acts much like nonreinforcing fillers, and no significant enhancement of physical properties is observed. Organic modification of the clay by replacing the interlayer metal cations by organoammonium or organophosphonium cations renders the hydrophilic surfaces of the silicate strongly organophilic.<sup>15,16</sup> In conventional clay-filled composite, the clay tactoids are held together by the interaction of anionic sites on the platelets with the interlayer metal ions. Exchange of the metal ions for the organic cations allows an increase in the interlayer separation and allows resin to penetrate between the galleries. The organic modification is observed as an increase in the interlayer spacing. Ideally, the organic modification should allow the complete separation of the tactoids, exfoliation, to create a dispersion of the platelets. In general, it is achievement of the exfoliated state that is essential for physical property enhancement to be achieved.<sup>17</sup> This exfoliated state is shown to enhance physical properties, such as a reduction in solvent uptake by epoxy<sup>18</sup> and improved thermal stability.<sup>19</sup> The clay platelets create a tortuous pathway for the diffusing molecules and inhibits water or oxygen molecules uptake. The more complex route reduces the rate of solvent uptake.

Correspondence to: R. A. Pethrick (r.a.pethrick@strath.ac.uk).

A number of factors can be considered to influence the degree of exfoliation, and include the choice of the clay added to the system and conditions used in the sample preparation, such as sonication and cure temperature.<sup>19,20</sup> Organic modification of montmorillonite increases the probability of complete exfoliation by altering the character of the gallery.<sup>21</sup> There is now a range of organic modifications of the base clay commercially available, and these impart different properties to the material in terms of its ease of exfoliation. The alkyl chain creates a more organophilic environment, and the long chains create space between the clay sheets for the monomer to percolate. The organically modified clay will have a greater affinity than the unmodified clay to exfoliate. The nature of the organic modification will influence the free energy of the clay surface and hence the thermodynamics of the clay–monomer–polymer interactions. The enhancement characteristics have been shown to vary with the type of organic modification that is used.<sup>22</sup> The presence of the alkyl ammonium ions catalyze polymerization within the clay galleries,<sup>23,24</sup> influencing the balance between the rate of polymerization inside and outside the clay galleries. A balance between these reactions is crucial for achieving higher degrees of exfoliation; if extragallery polymerization exceeds the reaction within the clay layers, only intercalation will occur. This catalytic effect due to the presence of organoclay has been examined through dynamic torsional vibration methods<sup>25–27</sup> and is reported to decrease gel time with increased clay loading. Becker et al.<sup>28</sup> also found that, when comparing epoxies, the system that was least influenced in reactivity with the addition of the organoclay resulted in least improvement in *d*-spacing relative to neat clay.

Diffusion of curing materials, both epoxy and hardener, between the clay layers is vital for promoting effective exfoliation. Use of higher cure temperatures<sup>26,27</sup> provide sufficient thermal energy to promote the exfoliation process; however, excessive temperatures can result in dissociation of the alkyl ammonium ions and hence influence the surface energy of the clay relative to that of the monomer–polymer system.<sup>29</sup>

Sonication has been shown to be an effective method for dispersing particles.<sup>30–32</sup> Lam et al.<sup>33</sup> found that although sonication had little effect on the interplanar distance between nanoplatelets, it did affect the size of nanoclusters of clay in the epoxy nanocomposite. This observation confirms previous observations by the authors on simple epoxy systems.<sup>20</sup> In previous articles, we have identified the advantages of the use of ultrasonic irradiation as a means of achieving a high degree of exfoliation of the clay in the monomers before the cure reaction.<sup>20,34</sup> It was also observed that the nature of the epoxy system influenced the property enhancement observed, indi-

cating the importance of the resin–clay interactions in determining physical properties.

Through the addition of clay nanocomposites to the epoxy resin, an improvement in the glass transition temperature is often observed.<sup>35,36</sup> There are a number of conjectured explanations for this phenomenon. Lu and Nutt<sup>35</sup> observed slower segmental relaxations, attributed to the polymer chains being anchored to the surface of the clay. The presence of the clay has also been found to promote a more fully cured system, resulting in the relaxation process covering a wider temperature range, which would also result in an increased glass transition temperature.<sup>36</sup> Other studies have found that the addition of clay nanocomposites can result in a reduction the glass transition temperature, often attributed to an increase in free volume.<sup>22,28</sup> Chen et al.<sup>37</sup> however attributed the phenomenon to the formation of an interphase, the epoxy plasticized by the surfactant.

The aim of this current study was to establish how ultrasonication, the nature of the curing agent, the moisture content of the clay, and the temperature used in the cure process influence the physical properties that are achieved with a particular nanocomposite system. Previous studies<sup>20,22,34</sup> have indicated that for epoxy resin system the use of Cloisite 30B yields physical property enhancement with a low viscosity aliphatic curing agent. This study has therefore been restricted to the study of this one type of clay. In this study, we report data on the effects on a conventional high-temperature aromatic amine-based cure system and the effect of change in the nature of the epoxy resin. The two most conventional epoxy resins available are based on bisphenol A and F, and both are examined in this article.

## EXPERIMENTAL

### Materials

The epoxy resin, diglycidylether of bisphenol A (DGEBA) was supplied by Ciba Specialty Chemicals (Araldite resin, MY 750), Diglycidyl ether of bisphenol F (DGEBF) was provided by Vantico Ltd. The hardener 4,4-diaminodiphenylmethane (DDM) supplied by Aldrich Chemicals was used as supplied. The epoxy resin nanocomposites were prepared using a stoichiometric ratio of 100 : 14.2 (w/w) epoxy resin: hardener. The hardener 4,4'-diaminodiphenylsulphone (DDS) supplied by Aldrich Chemicals was used as supplied. The organically modified montmorillonite clay used in this study was Cloisite<sup>®</sup> 30B, supplied and characterized by Southern Clay. The clay is organically modified using bis(2-hydroxy-ethyl) methyl T ammonium. The T represents tallow, which is a natural product composed predominantly of unsaturated C<sub>18</sub> (65%), C<sub>16</sub>(30%), and C<sub>14</sub>(5%) alkyl chains. The number of

milli-equivalents of the ammonium salt used per 100 g of montmorillonite during the cationic exchange reaction with the sodium montmorillonite precursor is 90. This intercalated material has an intergallery spacing  $d_{100}$  of 18.56 Å. The resin formulations examined correspond to DGEBA/DDM 100:14.2 (w/w) epoxy resin: hardener; DGEBA/DDS 100:17.7 (w/w) epoxy resin: hardener (0.54 equiv) and DGEBF/DDS 100:30.2 (w/w) epoxy resin: hardener (0.8 equiv). Chemicals used are illustrated in Figure 1.

### Cure of resin systems

#### DGEBA + DDS/DDM

A known amount of Cloisite was added to 50 g DGEBA at 80°C, stirred, and then sonicated with stirring for 15 min using a Cole-Palmer Ultrasonic Processor (model CPX 750) coupled to 6.35 mm tapered probe. The resulting suspension was maintained at 80°C and sonicated with stirring for another three periods of 15 min during 24 h before adding the required amount of DDS. The mixture was sonicated with stirring for 10 min until the DDS dissolved. The solution was now degassed and poured into a preheated mold and cured for a preset time and temperature.

#### DGEBF/DDS

A known amount of Cloisite 30B was added to 50 g DGEBF at 80°C, stirred then sonicated with stirring for 15 min using a Cole-Palmer Ultrasonic Processor (model CPX 750) coupled to 6.35 mm tapered probe. DDS was subsequently added to the epoxy/clay mixture and heated for 50 min at 120°C. The solution was now degassed and poured into a preheated mold and cured for a preset time and temperature.

### Rheology

Measurements were carried out on an AR-1000 rheometer (TA Instruments, Crawley, UK) using cone

and plate geometry with a truncated 4-cm, 2° steel cone. Measurements were made in steady shear over a range of shear rate 0.3–1300 s<sup>-1</sup> and in oscillatory shear over a range of frequency 0.1–100 rad/s. All experiments were performed at a temperature of 80°C, and were repeated at least three times on at least two separate samples of each suspension.

### Strathclyde rheometer

A small sampled of DGEBF/DDS/Cloisite 30B mixture was removed during sample preparation and placed in a glass vial that was subsequently positioned in a preheated Strathclyde rheometers.<sup>38,39</sup> The data was collected via a computer program, Picolog<sup>TM</sup>.

### X-ray diffraction

X-ray samples were examined using a Siemens Diffraktometer D500 with copper wavelength. The epoxy nanocomposite plaque was placed in the sample holder and data recorded through angles from 1.5° to 8° with a step-size of 0.02 and dwell time of 4 s.

### Dynamic mechanical thermal analysis

DMTA measurements were made using a Polymer Laboratories Dynamic Mechanical Thermal Analyser MKIII, at a frequency of 1 Hz, a strain of  $\times 4$ ; scanning rate of 4°C per minute and the samples were clamped with a torque of 40 N.

### Transmission electron microscopy experiments

A Reichart-Jung Ultracut-E microtome with a diamond knife at a cutting angle of 5°, at 1.5 mm/s was used to obtain sections with a thickness of 60–70 nm. The sections were floated on water and collected for inspection on a copper mesh and the water allowed to evaporate. TEM images were obtained using a 80 kV

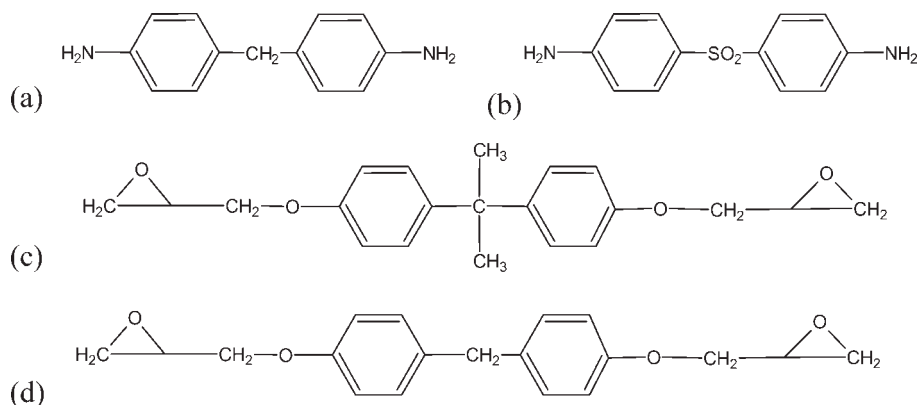


**Figure 1** (a) Diamino diphenyl methane (DDM); (b) diamino diphenyl sulfone (DDS); (c) diglycidyl ether of bisphenol A (DGEBA); (d) diglycidyl ether of bisphenol F (DGEBF).

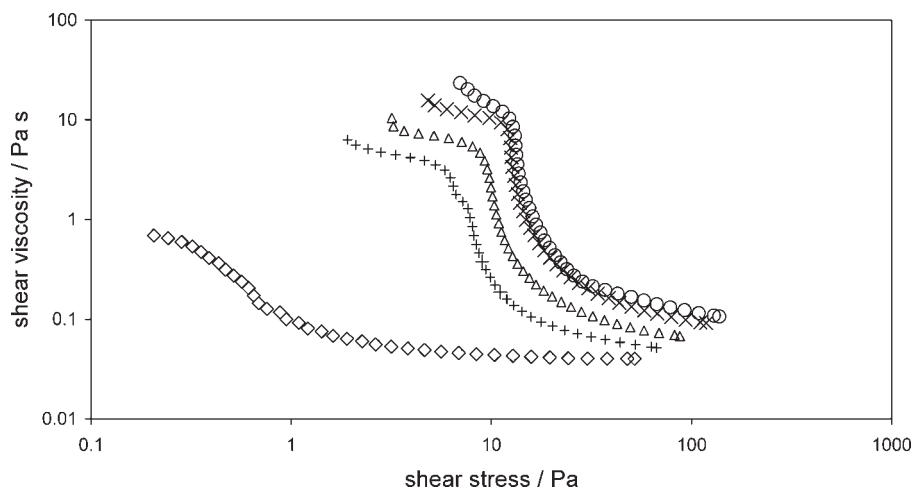


**Figure 2** Viscosity versus shear stress illustrating changes in flow curves with increased sonication duration for a 4% dispersion of clay in epoxy at 80°C. ( $\diamond$ ) 0 min; (+) 5 min; ( $\triangle$ ) 10 min; ( $\times$ ) 20 min; and ( $\circ$ ) 30 min of sonication time.

Zeiss-902 electron microscope. Note that no residual image was observed.

## RESULTS AND DISCUSSION

The study was divided into an examination of the processes associated with the exfoliation of the clay and evaluation of the physical property changes resulting from the incorporation of the clay in the cured polymer matrix.

### Factors influencing the exfoliation process in the epoxy monomer

#### Sonication

In previous articles,<sup>20,34</sup> we have demonstrated that exfoliation can be aided by the use of ultrasound.

Determination of the extent of exfoliation in a fluid is difficult using conventional X-ray methods, and it was shown that the shear rate dependence of the viscosity provides a useful tool to study the nature of the dispersion of the clay platelets prior to the cure process.

It is appropriate to consider the influence of various factors on the exfoliation process prior to study of the cured systems.

*Effect of clay loading and sonication time.* Monomer containing exfoliated clay possesses a high initial viscosity due to the formation by the clay platelets of the “house-of-cards” structure as a result of edge to face platelet interactions. The application of shear causes the platelets to become aligned in the flow direction and a resultant decrease in the viscosity is observed, Figure 2. The “house-of-cards” structures are associ-

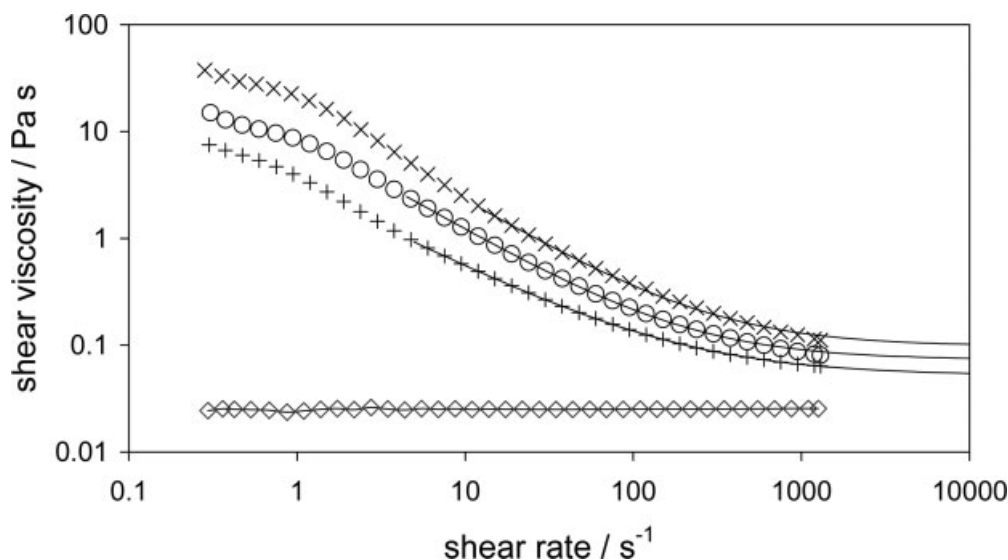


**Figure 3** Viscosity versus shear rate illustrating changes in flow curves with increased Cloisite 30B loading in epoxy monomer at 80°C. High shear rate data fitted to Sisko model. ( $\diamond$ ) 0 wt %; (+) 2 wt %; ( $\circ$ ) 4 wt %; ( $\times$ ) 6 wt %.

**TABLE I**  
Parameters Determined from Fitting the Data to a Herschel–Bulkley Model at Low Shear Rates, and a Sisko Model at High Shear Rates

Parameter	Concentration			
	0%	2%	4%	6%
$\tau$ (Pa)		0.316	0.278	0.256
$\eta_{\infty}$ (Pa/s)	0.0249	0.0522	0.0732	0.0981
$k_1$ (Pa/s)		1.24	2.92	5.26
$n$		0.219	0.091	0.077
$\sigma_0$ (Pa)		3.87	10.7	19.8
$k_2$ (Pa)		0.446	0.684	1.447
$m$		0.857	0.835	0.767
$\phi$	0	0.01	0.02	0.03
$\eta_{rel}$	1	2.097	2.940	3.940
$\eta_{sp}$	0	1.097	1.940	2.940

ated with edge to face stacking of platelets. This type of structure is favored as a consequence of electrostatic interaction between the negatively charged sites on the surface of the clay platelets and the positively charged sites located in the edges. The quarternary ammonium organic treatment will block certain of these negative sites, but sufficient will still remain to aid the formation of such a structure. The kinks in the viscosity shear stress plots are consistent with their being a critical yield condition for the “house-of-cards” structure.

These 3D structures will act like a network, but will exhibit a yield stress associated with the breaking of the electrostatic interactions. The initial dispersion of the clay in the epoxy resin shows a low level of exfoliation as indicated by the small rise in the viscosity at low shear rates. However, sonication of the epoxy resin/organoclay mixture for 5 min results in a significant increase in viscosity. Further sonication leads to an increase in the degree of exfoliation (Fig. 2), reaching a maximum viscosity after approximately 30 min. This suggests that with increasing sonication, the extent to which exfoliation is being achieved is increased. With high energy ultrasound, the possibility of cavitation exists and this can impart high temperatures locally as a result of the explosive decompression in the region of the bubbles being formed. In addition, it is also possible that the ultrasound can couple through relaxation mechanisms with the hydration sheath of water molecules bound to the surface of the platelets. Both mechanisms will aid the processes of exfoliation of the clay platelets. The exfoliated platelets can form the lower energy “house-of-cards” structure, which minimizes the interaction energy by ion pairing.

Interestingly, increasing the clay loading, as shown in Figure 3, leads to an increase in the viscosity for a constant sonication time, but is less dramatic than the effects of sonication time (Fig. 2). This reflects the increased ability to form a “house-of-cards” structure

with increasing concentration of clay in the material. With an addition of 6 wt % Cloisite 30B, a 15-fold increase in viscosity is observed, confirming the massive effects of exfoliation on the viscosity of the media. The high shear rate data has been fitted to a Sisko model,<sup>40</sup>  $\eta = \eta_{\infty} + k_1(\tau\dot{\gamma})^{n-1}$  where  $\eta_{\infty}$  is the viscosity at very high shear rate (when all structure has broken down),  $\tau$  is a relaxation time,  $n$  is a power law index, and  $k_1$  is a constant. The Sisko model provides a method of describing the relative rate of the reorientation of the clay platelets in the flow field. Movement of an isolated platelet in a viscous media (epoxy monomer) will be expected to be a function of the viscosity of the monomer. The values obtained for these parameters are shown in Table I.

The relaxation times have been estimated from the crossover frequency in the plots of storage ( $G'$ ) and loss ( $G''$ ) moduli as functions of angular frequency, as shown in Figure 4, and do not show marked concentration dependence. This observation is consistent with the premise that the primary process is associated with the breaking of the electrostatic contacts and alignment of the platelets in the flow field. A small shift to lower angular frequency with increasing viscosity of the mixture is consistent with the model.

Krisnamoorti and Silva<sup>41</sup> have presented similar rheological behavior as that shown in Figures 2 and 3. Their studies were performed on thermoplastic polymers, and the interpretation of the data is complicated by the presence of absorption of the polymer chains on the clay platelets, influencing the shear dependence of the viscosities observed.

In line with the work of Krisnamoorti and Silva,<sup>41</sup> the low shear rate data was fitted to a Herschel–Bulkley model<sup>42</sup>  $\sigma(\dot{\gamma}) = \sigma_0 + k_2(\tau\dot{\gamma})^m$ , where  $\sigma_0$  is a yield stress,  $\tau$  is a relaxation time,  $m$  is a power law index, and  $k_2$  is a constant. The yield stress may be associated with the multiple electrostatic interactions and is a direct consequence of the extended formation of a

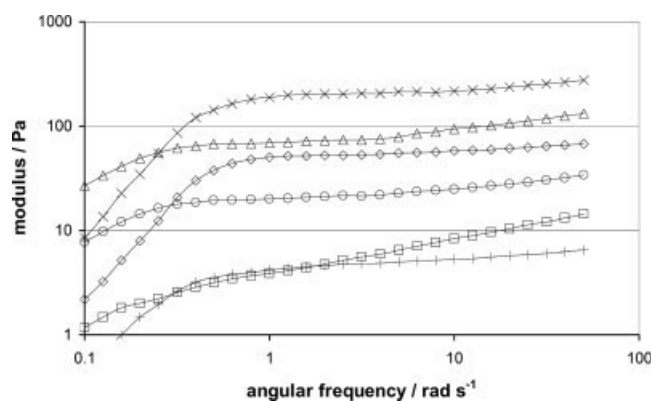


**Figure 4** Storage ( $G'$ ) and loss ( $G''$ ) moduli for each concentration 2 wt % (+,  $\square$ ); 4 wt % ( $\diamond$ ,  $\circ$ ); 6 wt % ( $\times$ ,  $\triangle$ ). The reciprocal of the crossover frequency is an estimate of the dominant relaxation time.

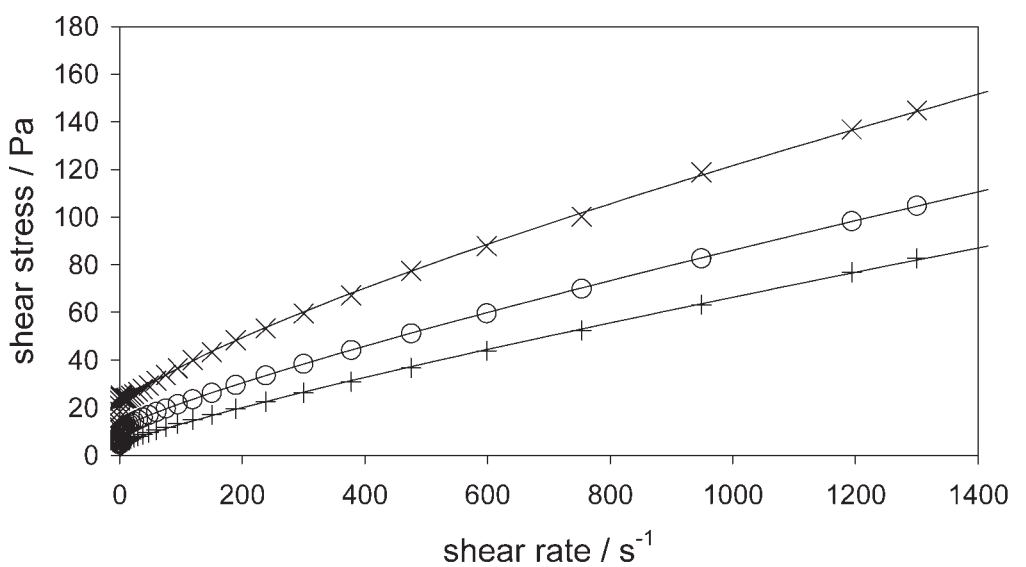
house of card structure throughout the fluid. Values are found in Table I, and the graph is shown in Figure 5(a). The very low shear rate part is shown in Figure 5(b), highlighting the yield stress.

The values estimated from this study can be compared with those published by Krishnamoorti and Silva<sup>41</sup> who reported values of 110 and 380 Pa for 6.7 and 9.5 wt % organo-montmorillonite loadings, (modified with dimethyldioctadecyl-ammonium) respectively. The values observed for this system are 3.87 Pa for 2 wt %, 10.7 Pa for 4 wt %, and 26.4 Pa for 6 wt %. These values are slightly different from those obtained by Krishnamoorti and Silva<sup>41</sup> and reflect the

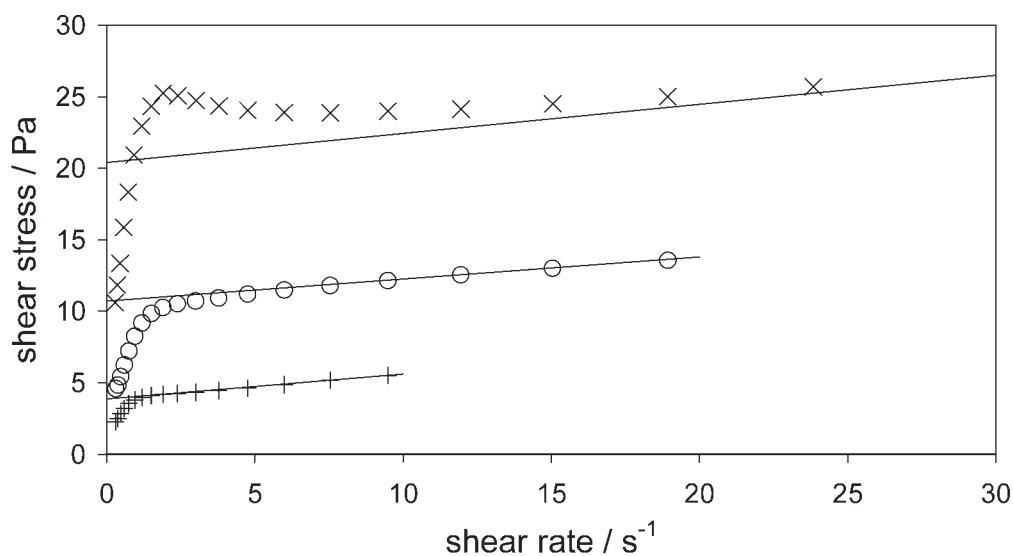
differences in electrostatic nature of the different clays used in the studies.

A plot of the values of the specific viscosity  $\left(\eta_{sp} = \frac{\eta_{sc} - 1}{\eta_s}\right)$ , where  $\eta_s$  is the viscosity of the continuous phase, versus the phase volume fraction,  $\phi$ , of clay gives a linear plot, the slope of which is 98.5 (see Fig. 6).

If the particles were spherical then this slope should have a value of 2.5.<sup>43</sup> However, for higher aspect ratio particles, such as the clay platelets, a higher value would be predicted,<sup>43</sup> as is found. The coefficients  $k_1$  in the Sisko model and  $k_2$  in the Herschel–Bulkley are also directly related to the platelet interaction. The



(a)



(b)

**Figure 5** Shear stress versus shear rate illustrating changes in flow curves with increased Cloisite 30B loading in DGEBF monomer, at 80°C. (+) 2 wt %; (O) 4 wt %; (x) 6 wt %. (a) Shows the complete range of shear rates, and (b) shows the yield stress at low shear rates.

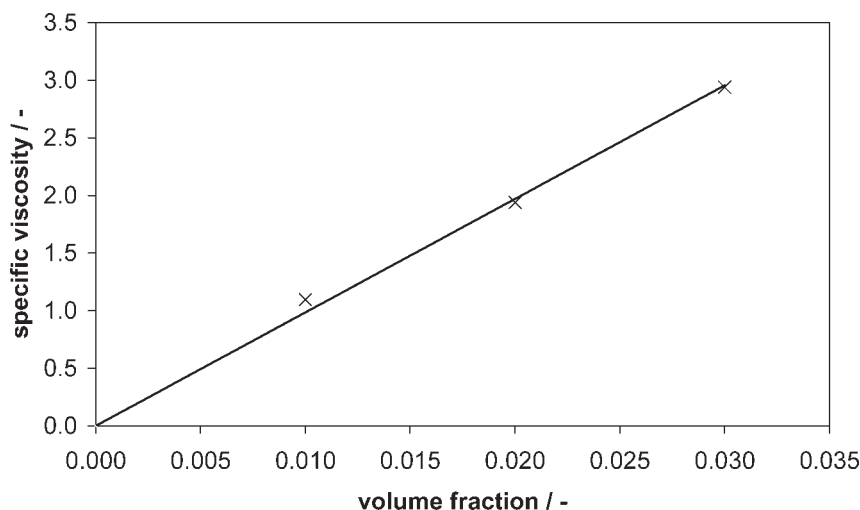


Figure 6 Viscosity versus volume fraction of cloisite 30B in epoxy.

values increase in a nonlinear function reflecting two factors. First, there is a critical concentration for volume fillings of the media by a “house-of-cards” structure, and this appears to be just below 2 wt % loading. Second, as the concentration increases, the number of contacts for platelets can increase, hence increasing the yield stress. The non linear concentration dependence of the yield stress  $k_1$  and  $k_2$  reflect the consequences of these multiple interactions.

*Effect of water content on the surface of the clay.* To investigate the effect of water molecules that are absorbed on the surface of the clay, a range of samples were prepared with clay having varying moisture contents. For this study, each sample of epoxy with 4 wt % Cloisite 30B was sonicated for 30 min. Clay equilibrated at 100% humidity by equilibration with atmospheric moisture for a prolonged period of time was designated “wet.” A sample of the clay was dried in an oven overnight at 105°C to provide the reference “dry” sample and showed a weight loss of 0.5 wt %. Mixing the “wet” and “dry” materials produced intermediate samples. The viscosity measurements show a distinct correlation between the amount of moisture present and the extent of exfoliation

observed, as measured by the viscosity at  $1.2 \text{ s}^{-1}$ . As shown in Figure 7, a near two-fold increase in viscosity occurs between the “dry” and “wet” samples. It is suggested that water is affecting the exfoliation by forcing the galleries apart either by being displaced from the surface by the higher temperatures created during decompression or by specific interaction through relaxation coupling with the hydration sheath of the water molecules bound to the clay surface. This has been found to be the case when applying microwaves rather than sonication. Aranda et al.<sup>44</sup> has observed that the microwaves activate water molecules, allowing effective intercalation of molecular organic compounds within the galleries of the organic modified clay system. This mechanism whereby the microwaves couple with the dipoles of the water molecules is directly analogous to the relaxation coupling possible with the hydration sheath of the water molecules bound to the clay.

#### Strathclyde rheometer

The Strathclyde rheometer<sup>38,39</sup> was designed to study the cure processes in filled thermoset systems, and is

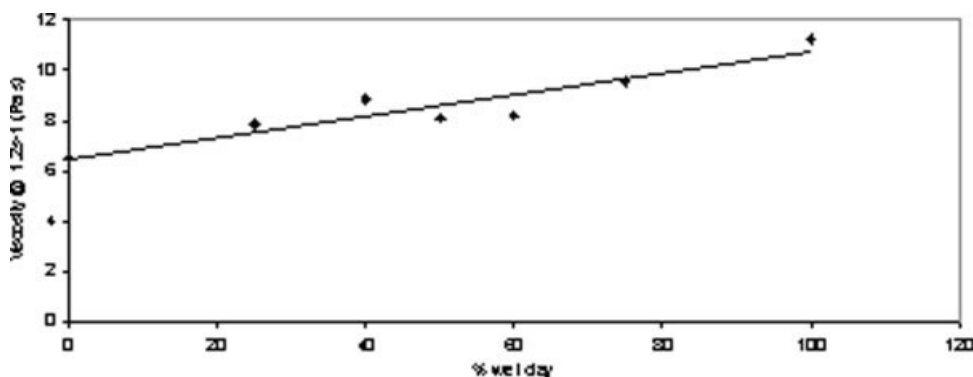
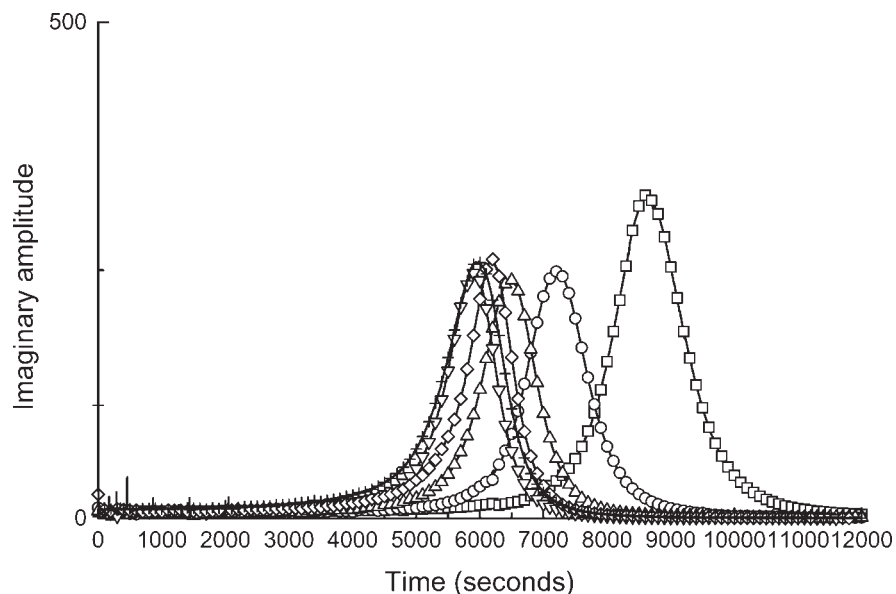


Figure 7 Viscosity at  $1.2 \text{ s}^{-1}$  versus % wet clay, showing increase in viscosity with increased moisture content of clay.



**Figure 8** Relative gelation points with increasing wt % Cloisite 30B, measured at 160°C. (□) 0 wt %; (○) 2 wt %; (△) 3 wt %; (▽) 4 wt %; (◇) 5 wt %; and (+) 6 wt % Cloisite 30B.

ideally suited to the study of the nanocomposites. It has been proposed by Chen et al.<sup>45,46</sup> that alkyl ammonium ions used to aid dispersion of the clay platelets can increase the rate of polymerization within the gallery. To investigate this effect, a range of samples were examined using the Strathclyde rheometer, with the Cloisite 30B content increasing from 0 to 6 wt % using both “wet” and “dry” starting materials. A decrease in the gel time was observed with increased clay content, Figure 8. A 15% reduction in gel time occurs with the addition of 2 wt % Cloisite 30B, with a further reduction in gel time with 4 wt % clay loading. However, further increases in clay loading above

4 wt % do not result in a further decrease in gel time; this is probably a consequence of the effects of diffusion on the propagation rates for the polymerization as a result of the high viscosities associated with the high clay loadings (Fig. 9).

The previous rheological studies indicated that the extent of the exfoliation was a function of the moisture content in the clay samples. Examination of the effect of moisture on the rates of cure (Fig. 10) indicates that the gel time decreases with increasing moisture content. At two different clay loadings, 2 and 5 wt %, a clear decrease in gel time is detected in the systems with clay containing a higher moisture content. The

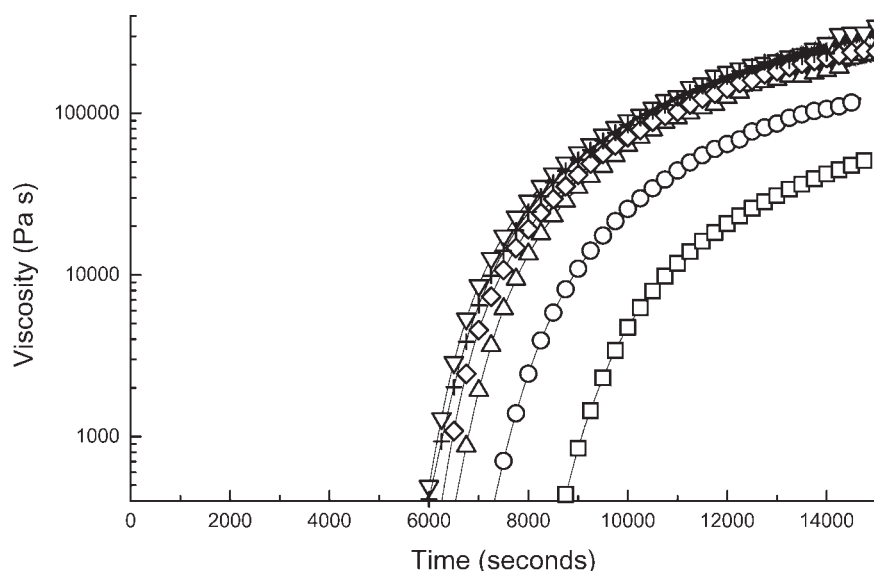


**Figure 9** Relative viscosity during cure with increasing wt % Cloisite 30B. (□) 0 wt %; (○) 2 wt %; (△) 3 wt %; (▽) 4 wt %; (◇) 5 wt %; and (+) 6 wt % Cloisite 30B.



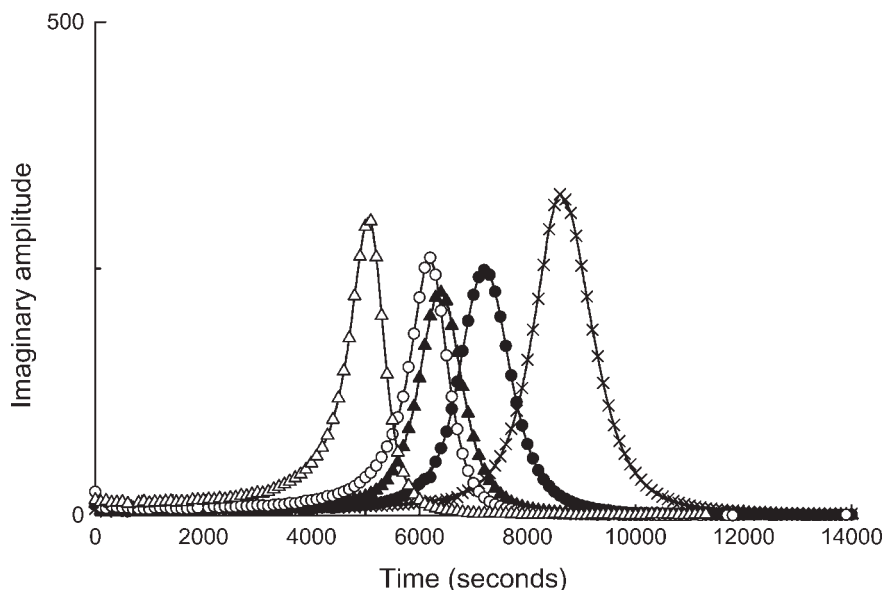


**Figure 10** Relative gelation points with varying moisture of clay added to epoxy, measured at 160°C. (x) 0 wt %; (●) 2 wt % dry; (▲) 2 wt % wet; (○) 5 wt % dry and (△) 5 wt % wet Cloisite 30B.

observed increase is consistent with their being a greater degree of exfoliation in the “wet” sample compared with the “dry” sample at the same clay loading. This relates to the rheological observations, an increase in the degree of exfoliation with increasing clay moisture (Fig 11). These results suggest that with increased exfoliation more alkyl ammonium ion sites are available to epoxy monomer, and therefore, there is an increase the rate of reaction within the galleries. These observations are consistent with those of Chen et al.<sup>45,46</sup>

#### Physical properties of the cured epoxy nanocomposites

The optimized dispersions of clay were cured thermally as indicated above. Plaques of material were produced and subjected to X-ray and dynamic mechanical thermal analysis (DMTA). The objective of this study was to examine the possible influence of change of the chemical structure of the epoxy resin on the changes in physical properties, which occur when the clay is incorporated to form the nanocomposite. The systems studied involve DEGBA, DGEBF, DDM,

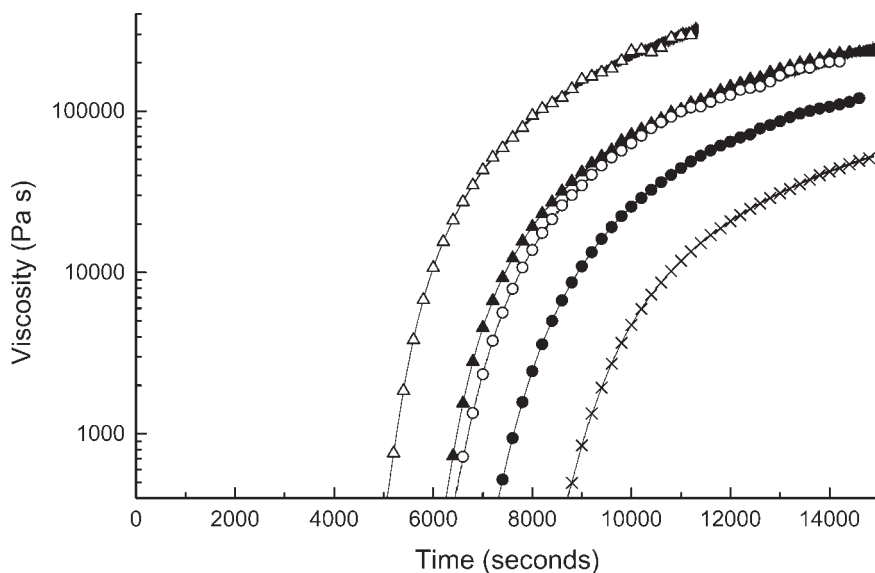


**Figure 11** Relative viscosity changes during cure with varying moisture of clay added to epoxy. (–) 0 wt %; (□) 2 wt % dry; (▲) 2 wt % wet; (○) 5 wt % dry and (▼) 5 wt % wet Cloisite 30B.

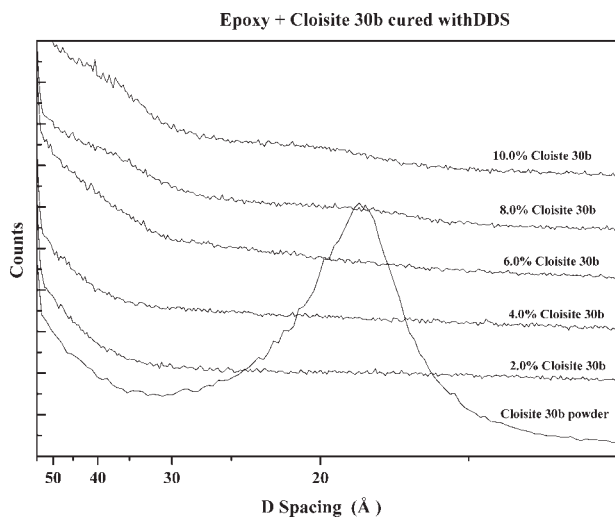


**Figure 12** Counts versus d spacing. XRD profile of DGEBA/DDM with increased clay loading.

and DDS. The molecular structures of these compounds are shown in Figure 1.

The DEGBA and DGEBF are intrinsically very similar except in terms of the bridge between the two phenyl rings. The  $(\text{CH}_3)_2\text{C}-$  group will place greater steric constraints on the phenyl group orientation than the less bulky  $-\text{CH}_2-$  linking group. Similarly, the  $-\text{SO}_2-$  bridging group in the DDS is sterically bulkier than the  $-\text{CH}_2-$  group in the DDM. These differences in structure influence the  $T_g$ , but will also influence the nature of the interactions that the resin can develop with the clay surface.

X-ray diffraction studies—*influence of concentration and cure temperature of degree of exfoliation*

To assess the degree of exfoliation, the X-ray diffraction spectra for the cured plaques were measured, Fig-

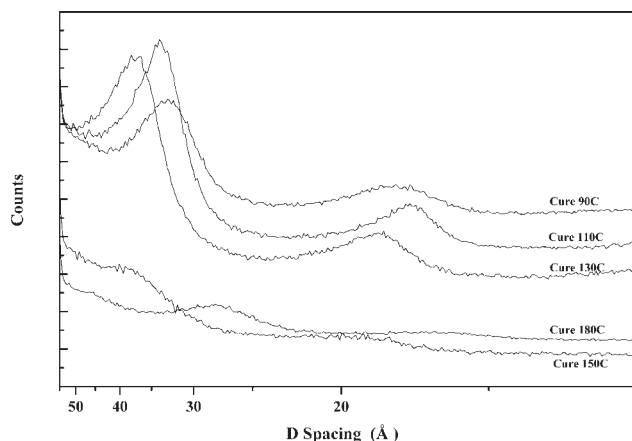


**Figure 13** Counts versus d spacing. Increased exfoliation with increase cure temperature. XRD profile of DGEBA/DDM + 8 wt % Cloisite 30B.

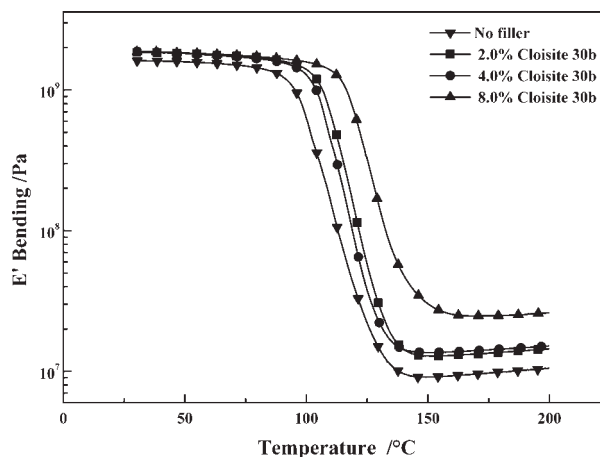


**Figure 14** Bending modulus versus temperature (DGEBA/DDM). Improved bending modulus in the rubber region with increased clay loading. ( $\nabla$ ) No filler; ( $\blacksquare$ ) 2 wt % Cloisite 30B; ( $\bullet$ ) 4 wt % Cloisite 30B; ( $\blacktriangle$ ) 6 wt % Cloisite 30B.

ure 12. XRD analysis of DGEBA/DDM with Cloisite 30B revealed the achievement of a high levels of exfoliation, up to a clay loading of approximately 8 wt % Cloisite 30B, after which increased intercalation was observed. Previous studies by Vaia and coworkers<sup>47,48</sup> and Balazs et al.<sup>49</sup> have indicated that the dispersion of the platelets at high concentrations will be influenced by similar factors to those that control alignment in liquid crystalline media. It is therefore to be expected that aligned structure should be detected at high concentrations as a consequence of these factors, the intergallery spacing being substantially greater than that achieved by the incorporation of the organic modifier. The observed X-ray diffraction behavior for these exfoliated samples are consistent with the predictions of Balazs et al.<sup>49</sup> It was also pointed out by

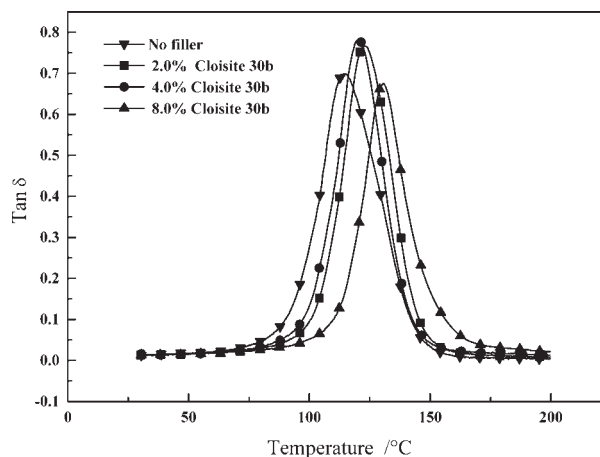


**Figure 15** Tan  $\delta$  versus temperature [DGEBA/DDM]. Increased glass transition temperature with increased clay loading. ( $\nabla$ ) No filler; ( $\blacksquare$ ) 2 wt % Cloisite 30B; ( $\bullet$ ) 4 wt % Cloisite 30B; ( $\blacktriangle$ ) 6 wt % Cloisite 30B.

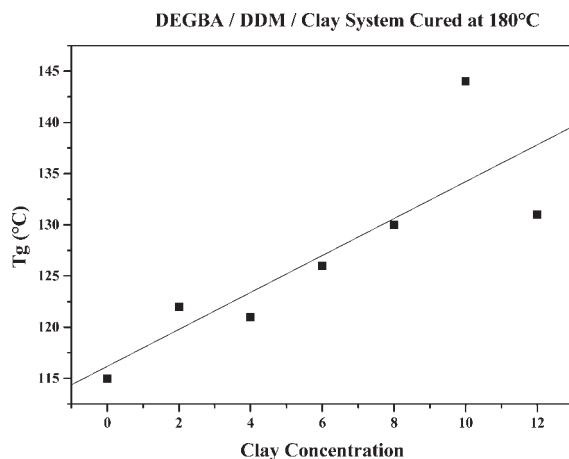


**Figure 16** Glass transition temperature versus clay concentration.

Balazs et al.<sup>49</sup> that the degree of exfoliation should vary with the interaction energy between the clay platelets and the resin matrix and this will be a function of temperature. X-ray studies of samples cured with DDS at different temperatures (Fig. 13) reveal that the higher cure temperature the greater the degree of exfoliation achieved. Increased temperature will provide increased thermal motion for the epoxy and harder to penetrate the clay galleries, and will also expand the gallery slightly further encouraging inter-gallery penetration. Polymerization between the clay platelets is crucial for achieving high levels of exfoliation as cured polymer increases the  $d$ -spacing of the galleries. This effect is observed with DGEBA/DDM and Cloisite 30B (Fig. 13)—higher cure temperatures produce XRD spectra with decreased peak intensity indicative of increased degrees of exfoliation.

In the case of the trace for the 12 wt % Cloisite 30B two peaks are observed at respectively, 40 and 20 Å. These peaks are associated with the same structure,

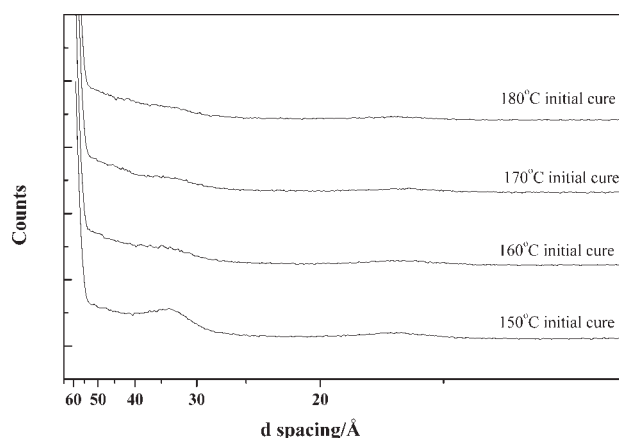


**Figure 17** Counts versus  $d$  Spacing. Higher degrees of exfoliation are achieved with higher cure temperatures in the DGEBA/DDM composite for 4 wt % clay.

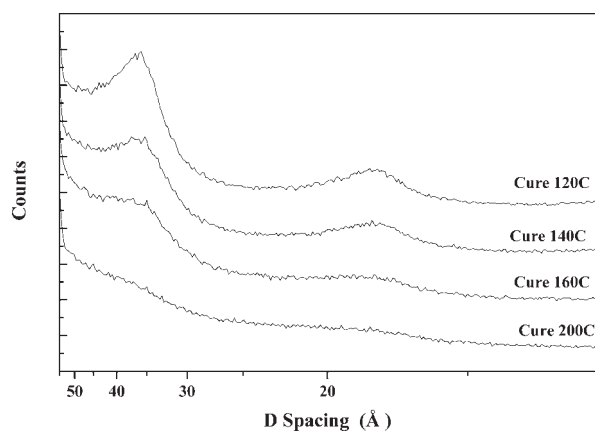


**Figure 18** Counts versus  $d$  Spacing. Higher degrees of exfoliation are achieved with higher cure temperatures in the DGEBA/DDS composite with 8 wt % clay.

and when a dominant peak is deflected at a long spacing, it is not unusual to see a second order reflection occurring at half the spacing. The peak at 20 Å should not be confused with the unexfoliated clay, which exhibits its first order peak at 18 Å. Similar features will be observed in the diffraction spectra for the other samples examined.

#### DGEBA and DDM nanocomposites

*Dynamic mechanical thermal analysis.* DMTA analysis of the DGEBA and DDM blend showed an increase in  $T_g$  with increase in concentration of Cloisite 30B, from a value of 115°C for the unfilled resin to a value of 140°C for the composite containing 12% clay. The modulus  $E'$  (Fig. 14) shows at low temperature a small increase with clay loading, reflecting the reinforcing action of the platelets (Fig. 15). In contrast the modulus measured above the  $T_g$  increased by a factor of 3 ( $1 \times 10^7 - 3 \times 10^7$ ) over the concentration range up to 12

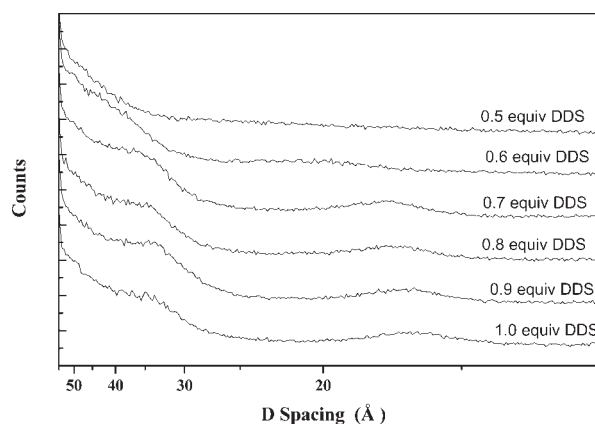


**Figure 19** Counts versus  $d$  Spacing. Higher degrees of exfoliation are achieved with lower quantities of cure agent for DDS with DGEBA.

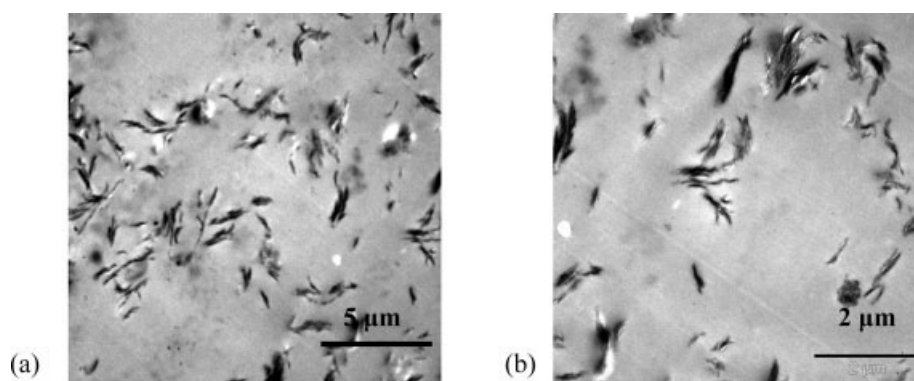


**Figure 20** TEM micrographs of DDS with DGEBF (a) 3000 $\times$  magnification (b) 7000 $\times$  magnification.

wt % Cloisite (Fig. 16). This increase in the elastic modulus reflects the reinforcing action due to the interaction of the polymer chains with the clay platelets. The interaction between the clay and the polymer acts as effective dynamic crosslinks in the system and produces the observed increase in the modulus.

The glass transition temperature is observed to vary approximately linearly over the range up to 8 wt %, averaging approximately 2 $^{\circ}$ C increase per 1 wt % clay added. The scatter in the data at higher concentrations may be attributed to the effects of the alignment of platelets to form the intercalated structures observed in the X-ray measurements (Fig. 12). There is a direct correlation between the increased effective elasticity as reflected in the high temperature values of  $E'$  (Fig. 14) and the shift in the  $T_g$  of the composite (Figs. 16 and 17). The increasing number of interactions, reflected in the  $E'$  values, between the resin and the clay leads to the increase in the values for the  $T_g$ .

#### DGEBF and DGEBA cured with DDS

*X-ray diffraction studies.* As with the DGEBA/DDM system both DGEBF and DGEBA with DDS experience a higher degree of exfoliation of the nanoclay with increasing cure temperature as indicated from X-ray diffraction spectra, Figure 18. Increasing the initial cure temperature results in an increase in the degree of exfoliation, as indicated by the decrease in peak height; complete exfoliation appears to have been achieved at 180 $^{\circ}$ C. Kong and Park<sup>11</sup> have proposed that in order for the epoxy and cure agent to have enough thermal motion to penetrate the clay galleries, the cure temperature must be maintained at a relatively high value. If the polymer and cure agent permeate the space between the platelets there will be a balance between inter and extragallery polymerization that will favor an increased degree of exfoliation, as observed in our experiments. Once more, secondary diffraction peaks are evident in the spectra for the lower cure temperatures.

Chin et al.<sup>50</sup> highlighted that the extent of cure can influence the separation of the clay platelets. In practice, epoxy resins are often cured with nonstoichiometric ratios, and to explore the possible effects of the epoxy/hardener a range of materials were produced with different cure agent equivalents, from 1.0 to 0.5 stoichiometric equivalents of DDS with DGEBF at a 4 wt % Cloisite 30B level. A clear pattern emerges from the X-ray diffraction data (Fig. 19). As the degree of cure decreases, the degree of exfoliation increases. With 0.5 and 0.6 equivalents of cure agent, there is no peak observed, indicating a high degree of exfoliation. As the cure increases to 0.7 equivalents, there develops a peak, which shifts to a smaller  $d$ -spacing with higher degrees of cure, indicating intercalation of the clay platelets. The observed effects can be attributed to an increasing amount of extra gallery polymerization taking place in the presence of a higher concentration of curing agent present in the mixture. Once again, the higher order peaks are observed for the samples that are closer to the stoichiometry.

*TEM images of the cured sample.* As a complementary experiment TEM images were obtained from the DGEBF, 0.8 DDS system and are presented in Figure

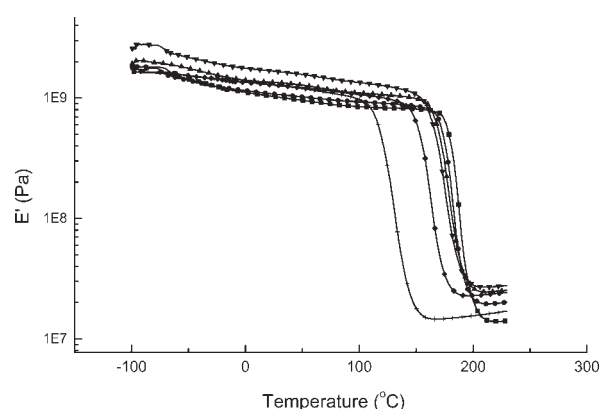


**Figure 21** (a) Bending modulus versus temperature. DGEBF + 4 wt % Cloisite 30B with varying level of cure DDS. (■) 1.0 equiv; (●) 0.9 equiv; (▲) 0.8 equiv; (▼) 0.7 equiv; (◆) 0.6 equiv; (+) 0.5 equiv.

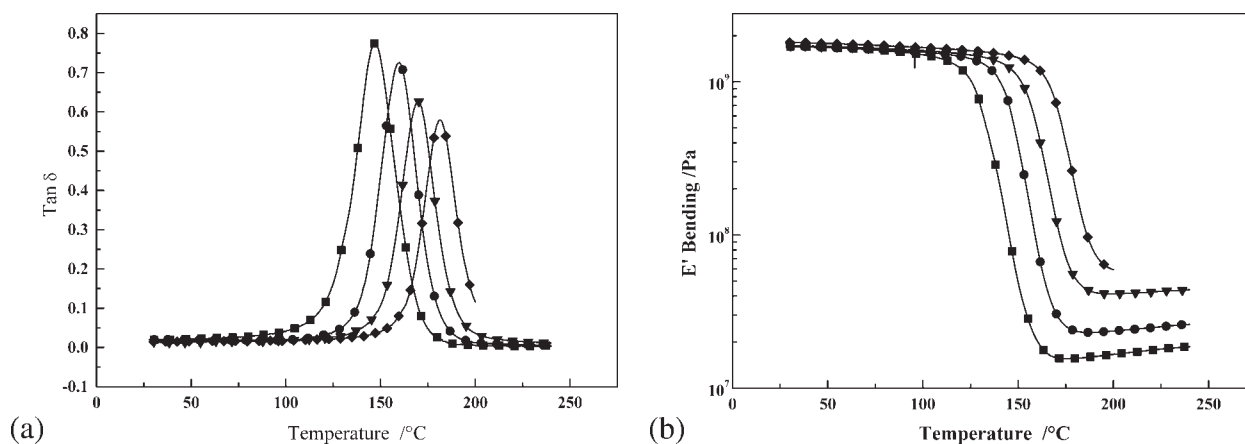


**Figure 22** (a) Tan  $\delta$  versus temperature (b)  $E'$  versus temperature for DGEBA/0.6 equivalents DDS cured at  $180^{\circ}\text{C}$  (■) No filler; (●) 2 wt % Cloisite 30B; (▼) 6 wt % Cloisite 30B; (◆) 10 wt % Cloisite 30B.

20. The images are similar to those presented by other researchers.<sup>51,52</sup> Although there are clearly platelets that are relatively close together, there is a fairly uniform distribution of material across the images. Closer inspection would indicate that in certain regions the clay platelets are adopting an intercalated structure, which is consistent with the X-ray data. There is also evidence of what appears to be individual exfoliated platelets, and these will have been responsible for the significant enhancement of the viscosity observed in the rheological measurements. TEM images are difficult to interpret, since they are a 2d section of a 3d distribution. The clay platelets have been sectioned in the microtoming process, and this may have slightly displaced them bringing adjacent plates closer together. The dimension of the platelets are similar to those reported by Liu et al.<sup>51</sup> and are of the order of 300–700 nm with intercalated clusters of the order of  $\sim 10$ –15 nm.<sup>52</sup>

*DMTA for DDS with DGEBA with different stoichiometry.* Figure 21 indicates that the  $T_g$  is dependent on the stoichiometric ratio used in the cure and changes from a value of  $134^{\circ}\text{C}$  for 0.5 equivalents to  $190^{\circ}\text{C}$  for 1.0 equivalent. The shift in the value of  $T_g$  with stoichiometric ratio is not a linear function of the ratio reflecting the effects of the different reactivity of the primary and secondary amine functions to form cyclic structures in the resin matrix. The change in the value of the  $T_g$  reflects the extent to which the changes in the formulation result in a different level of crosslink density in the matrix and parallel the effects, which are observed in the pure resin system.

*DMTA for DGEBA and DDS.* Figures 22–24 indicate that the  $T_g$  increased with increase in concentration of Cloisite 30b, from  $142^{\circ}\text{C}$  for the base resin to a value of  $185^{\circ}\text{C}$  at 10% Cloisite, approximately an increase of  $4^{\circ}\text{C}$  per addition of 1 wt % nanoclay. The X-ray diffraction data indicates that at the higher Cloisite concentrations, the Cloisite is intercalated. It is important

to recall that according to the model for the phase structure predicted by Balazs et al.<sup>49</sup> such a regular structure should exist at high clay concentrations.  $E'$  at low temperature showed a slight increase with increasing concentration, above  $T_g$ ,  $E'$  increased by a factor of 5 ( $1.2 \times 10^7 - 6.0 \times 10^7$ ) over the concentration range of 10% Cloisite as would be consistent with

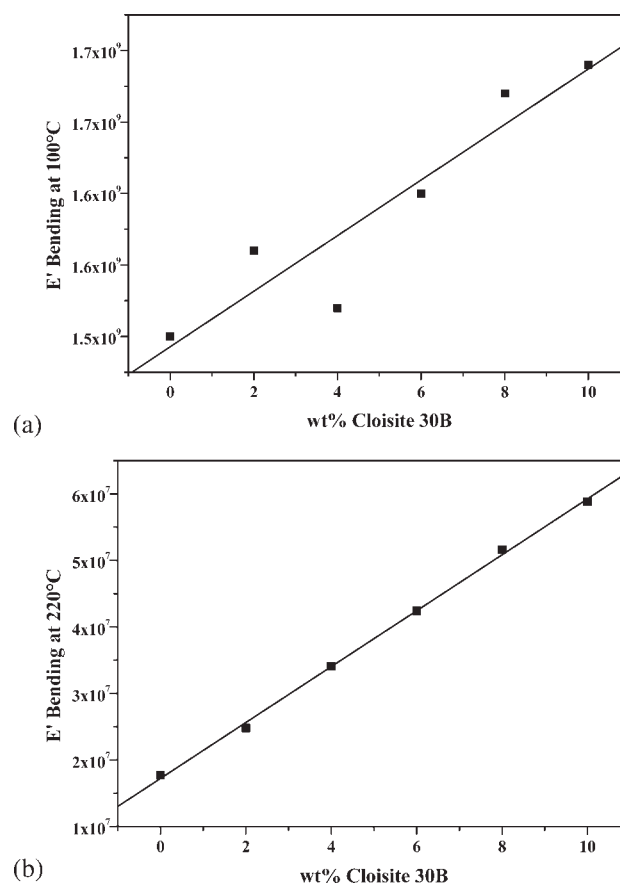


**Figure 23**  $E'$  bending versus clay concentration. Improvement in  $E'$  bending in (a) glassy region and (b) rubbery region with increased clay loading in DGEBA/DDS.

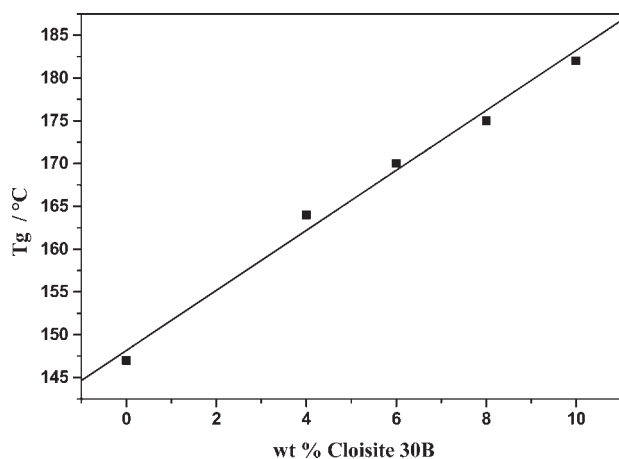


**Figure 24** Glass transition temperature versus clay concentration. Improvement in  $T_g$  with increased clay loading in DGEBA/DDS.

the predictions of an increasing interaction with the exfoliated clay platelets.

*X-ray diffraction data for DDS with DGEBF with different clay loadings.* For studying the effect of increasing the quantity of clay added to the matrix, a series of samples were prepared with clay loadings from 0 to 6 wt %. The X-ray diffraction data are presented in Figure 25. Complete exfoliation was achieved for the low levels of clay loading; however, as the loading was increased once more, a peak was observed reflecting the existence of intercalated clay with an enhanced spacing. The peaks amplitude increases with increasing clay concentration. There also appears to be a shift in the peaks, which varies with clay weight percentages. This shift is in the order of angstroms, which may infer changes in crosslink density of the polymer with variation in clay loading.

*DMTA of the DGEBF with DDS system.* DMTA measurements were performed for the DGEBF/DDS system cured at 160°C and the clay concentration was

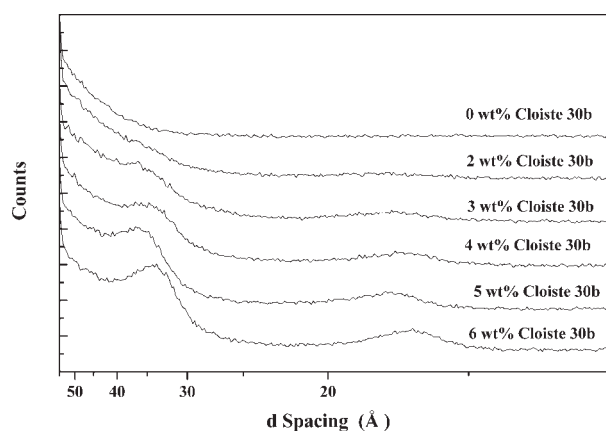


**Figure 25** Number of counts versus d spacing with increased clay loading for the DDS with DGEBF cured at 160°C.

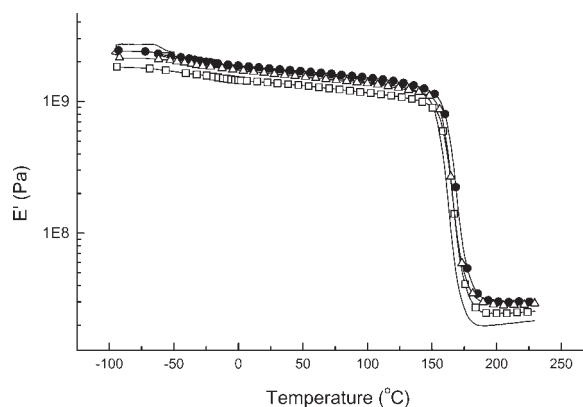


**Figure 26**  $E'$  bending versus temperature. Little improvement of physical properties is seen with increased clay loading in DGEBF/DDS. (—) No filler; (□) 2 wt % Cloisite 30B; (●) 4 wt % Cloisite 30B; (△) 6 wt % Cloisite 30B.

varied from 0 to 6 wt %, (Fig. 20) In contrast to the DGEBA/DDS system, DGEBF with DDS results in relatively very small improvements in both the glass transition temperature and bending modulus (Fig. 26). The value of  $T_g$  increasing from 165°C, for the base resin, to 168°C, for the 6 wt % filler composite, only an increase of 0.5°C per 1 wt % nanoclay (compared to a 4°C increase in  $T_g$  per 1 wt % cloisite 30B in DGEBA/DDS system).

Both the variation in the low temperature value of the  $E'$ , the high temperature value of  $E'$  and  $T_g$  with clay loadings are consistent with the DGEBF restricting the interactions of the polymer with the clay and have less of the reinforcing effects. This observation implies that subtle changes in the polymer–clay interaction can have profound effects in the resulting new composite.

## CONCLUSIONS

From rheological studies, it has been shown that sonication during preparation of epoxy nanocomposites is an effective method of dispersing the organically modified clay platelets. The observation of intercalated structures at high concentrations of the clay platelets is consistent with the predictions of the phase diagrams of Balazs et al.<sup>49</sup> The observation of the increased intergallery separations may be attributed to the clay having been exfoliated and then forming order intercalated structures. Analysis of the ease of exfoliation of “wet” and “dry” clay indicates that the thermal activation of water molecules in the galleries can aid the exfoliation process, and this is consistent with the observations of the action of microwaves in aiding exfoliation.<sup>44</sup> It has previously been proposed by Becker et al.<sup>36</sup> that the degree of exfoliation depends on the level of crosslinking. These studies would indicate that the value of  $T_g$  can be enhanced through additional interactions between the clay pla-

telets and the resin matrix. The value of the  $T_g$  appears to be determined by the extent of cure of the resin matrix. Change of the cure temperature alters the rates of polymerization and the clay–resin interaction, which results in an apparent high level of exfoliated clay platelets as indicated by the X-ray data. It is interesting that changing the flexibility of the bridging group between the phenyl moieties produces a significant effect on the  $T_g$  enhancement. When the three systems studied are compared, the greatest enhancement from the addition of cloisite 30B was found in the DGEBA/DDS system, 4°C improvement per wt % clay, followed by DGEBA/DDM then DGEBA/DDS (2 and 0.5 °C increase per wt % clay, respectively). The system DGEBA/DDS has the bridging groups, which are relatively bulkier (see Fig. 1), and experiences the largest  $T_g$  enhancement through nanoclay addition. It may be suggested that if the polymer chains are tethered to the clay surface, then perhaps the chains are more rigid, feel the greatest reduction in chain mobility through this constraint, and therefore the largest glass transition temperature improvement. The epoxy and cure agents that are more mobile still retain some range of motion through this pinning effect and therefore do not experience as much of a  $T_g$  enhancement from the addition of clay nanocomposite.

These studies indicate the importance of ensuring that the clay platelets are efficiently exfoliated and also the relevance of understanding the possible effects of the phase diagrams on the physical properties of these materials, and how the chemical structure of the monomer influences the enhancement which can be achieved.

S. McIntyre acknowledges the support of EPSRC and Cytec Engineered Materials for their provision of a postgraduate scholarship for the period of this study. The support of IR in the form of a postdoctoral fellowship from EPSRC is also gratefully acknowledged.

## References

- Giannelis, E. P. *Adv Mater* 1996, 8, 29.
- Kickelbick, G. *Prog Polym Sci* 2003, 28, 83.
- Andrew, W. *Handbook of Thermoset Plastics*; William Andrew Publishing: Norwich, NY, 1998.
- Neilsen, L. E.; Landel, R. F. *Mechanical Properties of Polymers and Composites*; Marcel Dekker: New York, 1994.
- Burnside, S. D.; Giannelis, E. P. *Chem Mater* 1995, 7, 1597.
- Wang, Z.; Pinnavaia, T. J. *Chem Mater* 1998, 10, 3769.
- Gelfer, M. Y.; Song, H. H.; Liu, L. Z.; Hsiao, B. S.; Chu, B.; Rafailovich, M.; Si, M. Y.; Zaitsev, V. *J Polym Sci Part B: Polym Phys* 2003, 41, 44.
- Delozier, D. M.; Orwoll, R. A.; Cahoon, J. F.; Johnston, N. J.; Smith, J. G.; Connell, J. W. *Polymer* 2002, 43, 813.
- Choi, M. H.; Chung, I. J.; Lee, J. D. *Chem Mater* 2000, 12, 2977.
- Lan, T.; Pinnavaia, T. J. *Chem Mater* 1994, 6, 2216.
- Kong, D.; Park, C. E. *Chem Mater* 2003, 15, 419.
- Kornmann, X.; Lindberg, H.; Berglund, L. A. *Polymer* 2001, 42, 1303.
- Chen, B. *Br Ceram Trans* 2004, 103, 241.
- Usuki, A.; Kojima, Y.; Kawasumi, M.; Okada, A.; Fukushima, Y.; Kurauchi, T.; Kamigaito, O. *J Mater Res* 1993, 8, 1179.
- LeBaron, P. C.; Pinnavaia, T. J. *Chem Mater* 2001, 13, 3760.
- LeBaron, P. C.; Wang, Z.; Pinnavaia, T. J. *Appl Clay Sci* 1999, 15, 11.
- Jan, I. N.; Lee, T. M.; Chiou, K. C.; Lin, J. J. *Ind Eng Chem Res* 2005, 44, 2086.
- Becker, O.; Simon, G. P.; Varley, R. J.; Halley, P. J. *Polym Eng Sci* 2003, 43, 850.
- Lim, S. T.; Choi, H. J.; Jhon, M. S. *J Ind Eng Chem* 2003, 9, 51.
- Brown, J.; Rhoney, I.; Pethrick, R. A. *Polym Int* 2004, 53, 2130.
- Nigam, V.; Setua, D. K.; Mathur, N.; Kar, K. K. *J Appl Polym Sci* 2004, 93, 2201.
- Kint, D. S.; Seeley, G.; Gio-Batta, M.; Burgess, A. J. *Macromol Sci Phys* 2005, 1021.
- Shi, H. Z.; Lan, T.; Pinnavaia, T. J. *Chem Mater* 1996, 8, 1584.
- Lu, J. K.; Ke, Y. C.; Qi, Z. N.; Yi, X. S. *J Polym Sci Part B: Polym Phys* 2001, 39, 115.
- Xu, W. B.; He, P. S.; Chen, D. Z. *Eur Polym J* 2003, 39, 617.
- Dean, D.; Walker, R.; Theodore, M.; Hampton, E.; Nyairo, E. *Polymer* 2005, 46, 3014.
- Chen, C. G.; Khobaib, M.; Curliss, D. *Prog Org Coat* 2003, 47, 376.
- Becker, O.; Cheng, Y. B.; Varley, R. J.; Simon, G. P. *Macromolecules* 2003, 36, 1616.
- Park, J.; Jana, S. C. *Polymer* 2004, 45, 7673.
- Mason, T. J. *Sonochemistry*; Oxford Science Publications: Oxford, UK, 1999.
- Ryu, J. G.; Park, S. W.; Kim, H.; Lee, J. W. *Mater Sci Eng C Biomimetic Supramol Syst* 2004, 24, 285.
- Park, S. S.; Bernet, N.; de la Roche, S.; Hahn, H. T. *J Compos Mater* 2003, 37, 465.
- Lam, C. K.; Lau, K. T.; Cheung, H. Y.; Ling, H. Y. *Mater Lett* 2005, 59, 1369.
- McIntyre, S.; Kaltzakorta, I.; Liggat, J. J.; Pethrick, R. A.; Rhoney, I. *Ind Eng Chem Res* 2005, 44, 8573.
- Lu, H. B.; Nutt, S. *Macromolecules* 2003, 36, 4010.
- Becker, O.; Varley, R.; Simon, G. *Polymer* 2002, 43, 4365.
- Chen, J.-S.; Poliks, M. D.; Ober, C. K.; Zhang, Y.; Wiesner, U.; Giannelis, E. *Polymer* 2002, 43, 4895.
- Pethrick, R. A. *Rheological Measurements*; Chapman and Hall: London, 1998.
- Affrossman, S.; Collins, A.; Hayward, D.; Trotter, E.; Pethrick, R. A. *J Oil Colour Chem Assoc* 1989, 72, 452.
- Sisko, A. W. *Ind Eng Chem* 1958, 50, 1789.
- Krishnamoorti, R.; Silva, A. S. In *Polymer-Clay Nanocomposites*; Pinnavaia, T. J., Beall, G. W., Eds.; Wiley: Chichester, UK, 2000; pp 316–343.
- Herschel, W. H.; Bulkley, R. *Kolloid Z Z Polym* 1926, 39, 291.
- Tager, A. *Physical Chemistry of Polymers*; Mir Publishing: Moscow, 1978; p 459.
- Aranda, P.; Mosqueda, Y.; Perez-Capote, E.; Ruiz-Hitzky, E. *J Polym Sci Part B: Polym Phys* 2003, 41, 3249.
- Chen, D. Z.; He, P. S. *Compos Sci Technol* 2004, 64, 2501.
- Chen, D. Z.; He, P. S.; Pan, L. J. *Polym Test* 2003, 22, 689.
- Brown, J. M.; Curliss, D.; Vaia, R. A. *Chem Mater* 2000, 12, 3376.
- Fong, H.; Liu, W. D.; Wang, C. S.; Vaia, R. A. *Polymer* 2002, 43, 775.
- Balazs, A.; Ginzburgh, V. V.; Lyatskaya, Y.; Singh, C.; Zhulina, E. In *Polymer-Clay Nanocomposites*; Pinnavaia, T. J., Beall, G. W., Eds.; Wiley: Chichester, UK, 2000; pp 281–313.
- Chin, I. J.; Thurn-Albrecht, T.; Kim, H. C.; Russell, T. P.; Wang, J. *Polymer* 2001, 42, 5947.
- Liu, W.; Hoa, S. V.; Pugh, M. *Compos Sci Technol* 2005, 65, 2364.
- Becker, O.; Varley, R. J.; Simon, G. P. *Eur Polym J* 2004, 40, 187.